Asociación Argentina
de Mecánica Computacional

Mecánica Computacional Vol XXVIII, págs. 553-572 (artículo completo)
Cristian García Bauza, Pablo Lotito, Lisandro Parente, Marcelo Vénere (Eds.)
Tandil, Argentina, 3-6 Noviembre 2009

DYNAMIC STABILITY OF THIN-WALLED BEAMS WITH GRADED MATERIAL PROPERTIES

Sebastián P. Machado[a,b] **and Marcelo T. Piovan**[a,b]

[a] *Centro de Investigaciones de Mecánica Teórica y Aplicada, Universidad Tecnológica Nacional Facultad Regional Bahía Blanca, 11 de Abril 461, B8000LMI, Bahía Blanca. Argentina, {smachado,mpiovan}@frbb.utn.edu.ar, http://www.frbb.utn.edu.ar*

[b] *CONICET*

Keywords: Dynamic Stability, Thin-Walled Beams, Functionally Graded Materials

Abstract. The dynamic stability of functionally graded thin-walled beams allowing for shear deformability is investigated in this article. The structure is subjected to axial external dynamic loading. The analysis is based on a model that has small strains and moderate rotations that are formulated through the adoption of a second-order non-linear displacement field. Galerkin's and Bolotin's methods are employed with the scope to discretize the governing equations and to determine the regions of dynamic instability, respectively. Regions of instability are evaluated and are expressed in non-dimensional terms. The influence of the longitudinal vibration on the unstable regions is investigated. The numerical results show the importance of this effect when the forcing frequency approaches to the natural longitudinal frequency, obtaining substantially wider parametric instability regions. The effect of shear flexibility and axial inertia for beams with different cross-sections and different types of graded material are analyzed as well.

1 INTRODUCTION

Strategic and high technology industries, such as defense, aerospace or automotive industries are demanding new and advanced materials in order to increase the leadership in high competitive goods. A few decades ago, designers claimed for new materials combining in a single specimen, the good properties of different kind of materials. That is, for example, the stiffness, electrical conductivity and machinability of metals and the high strength, low density and high temperature resistance of ceramics. During the past ten or twelve years these kind of advanced materials are becoming no longer experimental specimens in laboratories but a well developed reality. Functionally graded materials (FGM) are just an example of such advanced materials. In this kind of materials the variation in percentage of the material constituents (normally ceramic and metal) can be arranged in such a way to create a new material with graded properties in spatial directions.

Many papers have been devoted to study shells and solids constructed with FGM such as the works carried out by Reddy and Chin (1998), Reddy (2000), Praveen and Reddy (1998), El-Abbasi and Meguid (2000) and Kitipornchai et al. (2004) among others. There are many interesting approaches to analyze slender structures. Each of these approaches offers different perspectives and useful modeling alternatives.

The recent works of Chakraborty et al. (2003), Goupee and Vel (2006) and Ding et al. (2007), Xiang and Yang (2008), Yang and Chen (2008) among others can be considered the most relevant for functionally graded straight beams. In these papers different laws defining the graded properties of the beams have been employed. The gradation laws can be of the exponential type or a power law or any other with "ad-hoc" purposes. Many of the aforementioned papers introduce a three dimensional or a two dimensional complex model. On the other hand, there are quite a few papers devoted to study functionally graded thin-walled beams.

The works of Oh et al (2003, 2005), Fazelzadeh et al (2007) and Fazelzadeh and Hosseini (2007) are among the few papers devoted to the mechanics of thin-walled beams constructed with functionally graded materials. The scope of these papers has been mainly directed towards the analysis of rotating beams and secondarily to the analysis of the thermo-elastic coupling effects associated with graded properties. The works of Oh et al (2003, 2005) are also devoted to the study of dynamic instability of cylindrical spinning beams.

The dynamic instability of elastic slender structures like beams, rods and columns, induced by parametric excitation has been investigated by many researchers. In the work of Nayfeh and Mook (1979) one can find extensive sources and literature on these topics. The problems of dynamic stability for various structural elements have been thoroughly introduced and analyzed by Bolotin (1964). This last treatise provides useful tools for further studies and analysis on dynamic instability of slender structures. Some of these tools were employed by Machado (2008), and Machado and coworkers (2005, 2007) to study different aspects of dynamic instability in thin-walled composite beams.

In spite of the practical interest and future potential of the thin-walled functionally graded beam structures, particularly in the context of aerospace and mechanical applications, the most of the contemporary and available research is focused to characterize the dynamic response behavior of beams with solid sections or, at least, beams modeled as long conical or cylindrical shells (Naj et al, 2008). Under these circumstances, it appears that, to the best of authors' knowledge, there is a lack of research paying attention to the problem of dynamic stability of thin-walled beams with graded properties and subjected to axial dynamic excitation. With this context in mind, the present paper is devoted to analyze the patterns of dynamic stability for a given model of thin-walled beam considering full-shear deformability.

The concept of full shear deformability is adopted (Cortínez and Piovan, 2006; Machado et al, 2007; Piovan and Cortínez, 2007) to mean the inclusion in a unified fashion of shear stress/strain effects due to bending (the most common) and warping due to non-uniform torsion. Constitutive equations for functionally graded properties are developed and appropriately included in the beam model.

The purpose of the present investigation is the determination of the regions of dynamic instability of thin-walled functionally graded beams subjected to axial excitation. The beams are subjected to different types of boundary restrictions. The influence on the unstable regions of different modeling features such as shear deformation, natural longitudinal vibration, types of constitutive law and load parameter is extensively analyzed.

2 MODEL DESCRIPTION

2.1 Equations of motion

In Figure 1 one can see the structural model for the thin-walled beam. The points of the structural member are referred to a Cartesian co-ordinate system $\{O: x,\bar{y},\bar{z}\}$ located at the centroid where the x-axis is parallel to the longitudinal axis of the beam while $\bar{y}$ and $\bar{z}$ correspond to the principal axes of the cross section. The axes y,z are parallel to the principal ones but having their origin at the shear center, i.e. the point C. Besides a circumferential co-ordinate system $\{A: x,s,n\}$ is defined in the middle contour of the cross-section. On the other hand, y_0 and z_0 are the centroidal co-ordinates measured with respect to the shear center.

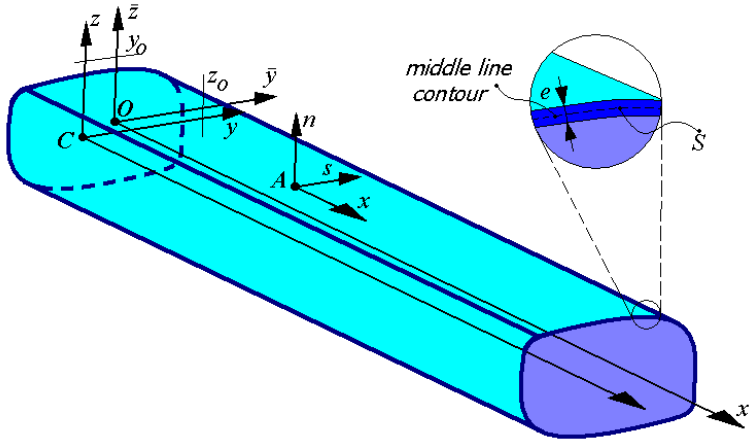

Figure 1: Structural model.

The mathematical model for the structure is based on the following hypotheses (Cortinez and Piovan, 2002; Machado and Cortínez, 2005):

a) The cross-section contour is rigid in its own plane.

b) Shell force and moment resultant corresponding to the circumferential stress σ_{ss} and the force resultant corresponding to the in-thickness strains γ_{ns} are neglected;

c) The radius of curvature at any point of the shell is neglected;

d) Twisting curvature of the shell is expressed according to the classical plate theory, but bending curvature is expressed according to the first order shear deformation theory; in fact, bending shear strain of the wall is incorporated;

e) The strains are considered small and the rotations are considered moderate.

In order to construct the model for thin walled beams with functionally graded properties the following hypothesis are added:

f) The properties are graded along the wall-thickness e according a prescribed law that is uniform around the contour domain S and depends only on the thickness variable n.

g) Shear effects across the wall-thickness e are neglected.

The laws of variation of the elastic and mass properties along the wall thickness can be prescribed in order to bear in mind for different types of material gradation such as metal to ceramic or metal (steel) to metal (aluminium). The properties can be defined to vary in continuous or layered fashion as well. With these properties it is possible to develop the constitutive equations in terms of stress resultants and generalized strains. This allows, in a single mathematical structure, the representation of isotropic, ceramic, functional and composite beams as well.

The motion equations for full shear deformable thin-walled beams can be written in the following form (Machado et al, 2007):

$$\begin{aligned}
&Q_x' + \overline{M}_1(x) = 0 \\
&-Q_y' - \left(Q_x v'\right)' + \overline{M}_2(x) = 0 \\
&M_z' - Q_y - \underline{Q_x z_0 \phi_x'} + \overline{M}_3(x) = 0 \\
&-Q_z' - \left(Q_x w'\right)' + \overline{M}_4(x) = 0 \\
&M_y' - Q_z + \underline{Q_x y_0 \phi_x'} + \overline{M}_5(x) = 0 \\
&-\left(T_w' + T_{sv}'\right) - \underline{\left(B_w \phi_x'\right)' + Q_x\left(z_0\theta_z' - y_0\theta_y'\right)} + \overline{M}_6(x) = 0 \\
&-B' + T_w + \overline{M}_7(x) = 0
\end{aligned} \tag{1}$$

Subjected to the following boundary conditions (at $x = 0, L$):

$$\begin{aligned}
Q_x - \overline{Q}_x = 0 \quad &or \quad \delta u = 0 \\
Q_y + Q_x v' = 0 \quad &or \quad \delta v = 0 \\
-M_z + \left(Q_x - \overline{Q}_x\right) z_0 \phi_x = 0 \quad &or \quad \delta\theta_z = 0 \\
Q_z + Q_x w' = 0 \quad &or \quad \delta w = 0 \\
-M_y - \left(Q_x - \overline{Q}_x\right) y_0 \phi_x = 0 \quad &or \quad \delta\theta_y = 0 \\
T_w + T_{sv} + B_w \phi_x' - \overline{Q}_x\left(z_0\theta_z - y_0\theta_y\right) = 0 \quad &or \quad \delta\phi_x = 0 \\
B = 0 \quad &or \quad \delta\theta_x = 0
\end{aligned} \tag{2}$$

In Eqs. (1) and (2), the apostrophes mean derivation with respect to the space variable x and time, respectively. The variable u is the axial displacement of the cross-section; v and w are the lateral displacements of the shear center. θ_y and θ_z are bending rotation parameters, ϕ_x is the twisting angle measured form the shear center and θ_x is a measure of the warping intensity. On the other hand, Q_X is the axial force; Q_Y and Q_Z are shear forces; M_Y and M_Z are bending moments, B is the bimoment, T_{SV} is the twisting moment due to pure torsion and T_W is the flexural-torsional moment due to warping torsion. B_W is a higher-order stress-resultant related to warping torsion that contributes to the torque (Machado and Cortínez, 2005). $\overline{Q}_x$ is the prescribed axial force acting at the boundaries. $\overline{M}_j$, $j = 1,...,7$ are the inertial forces.

2.2 Constitutive equations in terms of beam stress resultants

The beam forces mentioned in the previous paragraph can be defined in terms of the shell-stress resultants in the following form:

$$
\begin{aligned}
&Q_x = \int_S N_{xx} ds,\ B = \int_S \left[N_{xx}\omega_p - M_{xx} l(s) \right] ds, \\
&Q_y = \int_S \left(N_{xs} \frac{dY}{ds} \right) ds,\ \ Q_z = \int_S \left(N_{xs} \frac{dZ}{ds} \right) ds, \\
&M_y = \int_S \left(N_{xx}\overline{Z} + M_{xx} \frac{dY}{ds} \right) ds,\ M_z = \int_S \left(N_{xx}\overline{Y} - M_{xx} \frac{dZ}{ds} \right) ds, \\
&T_W = \int_S \left[N_{xs} \left(r(s) - \psi \right) \right] ds,\ T_{SV} = \int_S \left(N_{xs}\psi - 2M_{xs} \right) ds, \\
&B_W = \int_S \left[N_{xx} \left(Y^2 + Z^2 \right) - 2M_{xx} r(s) \right] ds
\end{aligned}
\tag{3}
$$

where ω_p is the warping function of the contour, ψ is the shear strain at the middle line, obtained by means of the Saint-Venant theory of pure torsion for isotropic beams, and normalized with respect to twisting angle gradient (Cortinez and Piovan, 2002; Machado and Cortinez, 2005). $\{Y,Z\}$ and $\{\overline{Y},\overline{Z}\}$ are the co-ordinates corresponding to points lying on the middle line of the wall measured from the shear center and the centroid, respectively. The functions $r(s)$ and $l(s)$ are defined as follows:

$$
r(s) = -Z(s)\frac{dY}{ds} + \mathrm{Y}(s)\frac{dZ}{ds},\ l(s) = Y(s)\frac{dY}{ds} + Z(s)\frac{dZ}{ds} \tag{4}
$$

The shell-stress resultants are described as:

$$
\begin{Bmatrix} N_{xx} \\ N_{xs} \\ M_{xx} \\ M_{xs} \end{Bmatrix} = \begin{bmatrix} \overline{A}_{11} & 0 & \overline{B}_{11} & 0 \\ 0 & \overline{A}_{66} & 0 & \overline{B}_{66} \\ \overline{B}_{11} & 0 & \overline{D}_{11} & 0 \\ 0 & \overline{B}_{66} & 0 & \overline{D}_{66} \end{bmatrix} \begin{Bmatrix} \varepsilon_{xx} \\ \gamma_{xs} \\ \kappa_{xx} \\ \kappa_{xs} \end{Bmatrix} \tag{5}
$$

where $\overline{A}_{ij}$, $\overline{B}_{ij}$ and $\overline{D}_{ij}$ are modified elastic coefficients, whose definitions can be obtained in terms of the longitudinal and transversal moduli and the Poisson coefficient by neglecting the hook force and hook moment of the shell (N_{ss} and M_{ss}) as one can see in the Appendix I. On the other hand, ε_{xx}, and γ_{xs} are normal and shear strains of the shell whereas κ_{xx} and κ_{xs} are the normal and transversal curvatures. As one can see there is no elastic coupling between normal and shear components. The functions $\overline{M}_j$, $j = 1,...,7$ are defined as follows:

$$
\begin{Bmatrix} \overline{M}_1 \\ \overline{M}_2 \\ \overline{M}_3 \\ \overline{M}_4 \\ \overline{M}_5 \\ \overline{M}_6 \\ \overline{M}_7 \end{Bmatrix} = \begin{bmatrix} J^{\rho}_{11} & 0 & 0 & 0 & 0 & 0 & 0 \\ & J^{\rho}_{11} & 0 & 0 & 0 & -z_0 J^{\rho}_{11} & 0 \\ & & J^{\rho}_{22} & 0 & 0 & 0 & 0 \\ & & & J^{\rho}_{11} & 0 & y_0 J^{\rho}_{11} & 0 \\ & & & & J^{\rho}_{33} & 0 & 0 \\ & Sym & & & & J^{\rho}_{00} & 0 \\ & & & & & & J^{\rho}_{44} \end{bmatrix} \begin{Bmatrix} \ddot{u} \\ \ddot{v} \\ \ddot{\theta}_z \\ \ddot{w} \\ \ddot{\theta}_y \\ \ddot{\phi}_x \\ \ddot{\theta}_x \end{Bmatrix} \tag{6}
$$

The dots over the variables intend for derivation with respect to the time, i.e. $(\dot{\bullet}) = d(\bullet)/dt$. The inertia coefficients J_{ij}^{ρ} are such that:

$$J_{ij}^{\rho} = \int_A \rho(n)\bar{g}_i\bar{g}_j dsdn, \text{ with } \bar{g} = \left\{1, \bar{Y} - n\frac{dZ}{ds}, \bar{Z} + n\frac{dY}{ds}, \omega_p(s) - nl(s)\right\}$$
$$J_{00}^{\rho} = \int_A \rho(n)\left(Y^2 + Z^2\right)dsdn \tag{7}$$

In order to clarify some aspects of the present model it should be mentioned that depending on the sort of hypotheses invoked into the displacement field employed to develop the model (normally first order formulation in displacements), some important terms may disappear as a consequence of the algebraic process, leading to incorrect expressions for the equations of motion and inaccurate predictions of the dynamic behavior of thin-walled beams. The underlined terms of the Eq. (1) are those that disappear in a first order formulation.

Under certain conditions, it can be shown (Machado et al, 2007) that the stress resultant B_W can be written in terms of the axial force Q_x (see Appendix I) leading to a more affordable solution procedure for the dynamic stability problem.

3 DYNAMIC STABILITY

3.1 Basic description

In this section the dynamic stability of a simply supported thin-walled composite beam is analyzed considering an axial excitation in the form:

$$P(t) = P_s + P_d Cos[\varpi.t] \tag{8}$$

where ϖ is the excitation frequency, $P_s = \alpha P_{cr}$, $P_d = \beta P_{cr}$, α is the static load factor, β is the dynamic load factor and P_{cr} is the critical load of the beam.

When the beam is excited in the axial (longitudinal) direction, and the interaction of this movement on the other motions has to be studied, the coupling of these various motions will depend on the symmetry of the cross-section analyzed.

The first differential equation shown in Eq. (1), that corresponds to the longitudinal movement can easily solved, disregarding the longitudinal inertia forces, in the following form:

$$Q_x = -P_s - P_d Cos[\varpi.t] \tag{9}$$

Although longitudinal inertia forces can substantially affect the dynamic stability of a beam only in the case where the frequency of the external force is near the longitudinal natural frequencies of the beam (i.e., when the longitudinal vibrations have a resonant character), however in this section and only for comparative purposes, the solution procedure is developed disregarding the longitudinal inertia forces. Once the expressions of the solution are attained, the effect of longitudinal inertia forces is afterwards accounted for.

The remaining differential equations can be discretized by means of the following wave functions:

$$\begin{array}{lll} v = v_o(t)Sin[\lambda_k x] & w = w_o(t)Sin[\lambda_k x] & \phi_x = \phi_{xo}(t)Sin[\lambda_k x] \\ \theta_z = \theta_{zo}(t)Cos[\lambda_k x] & \theta_y = \theta_{yo}(t)Cos[\lambda_k x] & \theta_x = \theta_{xo}(t)Cos[\lambda_k x] \end{array} \tag{10}$$

where $v_o(t)$, w_o(t), $\phi_{xo}(t)$, $\theta_{yo}(t)$, $\theta_{zo}(t)$ and $\theta_{xo}(t)$ are the associated displacement amplitudes

which are time dependent and

$$\lambda_k = \frac{k\pi}{L}, \quad k = 1,2,3,... \tag{11}$$

The formal substitution of Eq. (9) and Eq. (10) into the last six equations of Eq. (1) leads to a system of ordinary differential equations, which can be expressed in a compact form by using matrix notations as:

$$\boldsymbol{M}\ddot{\boldsymbol{U}} + \left(\boldsymbol{K} - P(t)\boldsymbol{S}\right)\boldsymbol{U} = \boldsymbol{O} \tag{12}$$

where:

$$\boldsymbol{U} = \left\{v_o, \theta_{zo}, w_o, \theta_{yo}, \phi_{xo}, \theta_{xo}\right\}^T \tag{13}$$

$$\boldsymbol{M} = \begin{bmatrix} J_{11}^{\rho} & 0 & 0 & 0 & -z_o J_{11}^{\rho} & 0 \\ & J_{22}^{\rho} & 0 & 0 & 0 & 0 \\ & & J_{11}^{\rho} & 0 & y_o J_{11}^{\rho} & 0 \\ & & & J_{33}^{\rho} & 0 & 0 \\ & sym & & & J_{00}^{\rho} & 0 \\ & & & & & J_{11}^{\rho} \end{bmatrix} \tag{14}$$

$$\boldsymbol{S} = \begin{bmatrix} \lambda_k^2 & 0 & 0 & 0 & -z_o\lambda_k & 0 \\ & 0 & 0 & 0 & 0 & 0 \\ & & \lambda_k^2 & 0 & y_o\lambda_k & 0 \\ & & & 0 & 0 & 0 \\ & sym & & & \lambda_k^2 J_{19}^E / J_{11}^E & 0 \\ & & & & & 0 \end{bmatrix} \tag{15}$$

$$\boldsymbol{K} = \begin{bmatrix} J_{55}^E\lambda_k^2 & -J_{55}^E\lambda_k & J_{56}^E\lambda_k^2 & -J_{56}^E\lambda_k & J_{57}^E\lambda_k^2 & -J_{57}^E\lambda_k \\ & J_{33}^E\lambda_k^2 + J_{55}^E & -J_{56}^E\lambda_k & J_{56}^E & -J_{57}^E\lambda_k & J_{57}^E \\ & & J_{66}^E\lambda_k^2 & -J_{66}^E\lambda_k & J_{67}^E\lambda_k^2 & -J_{67}^E\lambda_k \\ & & & J_{22}^E\lambda_k^2 + J_{66}^E & -J_{67}^E\lambda_k & J_{67}^E \\ & sym & & & \left(J_{88}^E + J_{77}^E\right)\lambda_k^2 & -J_{77}^E\lambda_k^2 \\ & & & & & J_{44}^E\lambda_k^2 - J_{77}^E \end{bmatrix} \tag{16}$$

$\boldsymbol{M}$, $\boldsymbol{S}$ and $\boldsymbol{K}$ are the mass matrix, geometric stiffness matrix and elastic stiffness matrix, respectively. Definitions of constants J_{ij}^E are detailed in Appendix I.

From Eq. (12) one can obtain the solution to different problems. Then, the problem concerning the determination of frequencies of free vibration of a beam loaded by a constant longitudinal force can be expressed as:

$$\left|\boldsymbol{K} - P_s\boldsymbol{S} - \Omega^2\boldsymbol{M}\right| = 0 \tag{17}$$

while the problem of the determination of frequencies of free vibration of an unloaded beam leads to the following equation:

$$\left|\boldsymbol{K} - \Omega^2\boldsymbol{M}\right| = 0 \tag{18}$$

and the buckling problem can be analyzed from the following equation:

$$\left|\boldsymbol{K} - P_s \boldsymbol{S}\right| = 0 \tag{19}$$

3.2 Principal parametric resonance

The unstable boundaries for the thin-walled composite beam subjected to an axial periodic load are studied in this section. In the classification of parametric resonance, if ϖ is the excitation frequency and Ω_i the natural frequency of the ith mode, parametric resonance of "first kind" is said to occur when $\varpi/2\Omega \approx 1/r$, r = 1,2,…while parametric resonance of the "second kind" is said to occur when $\varpi/(\Omega_k \pm \Omega_j) \approx 1/r$, r = 1,2,…($k \neq j$). In both cases the situation where r =1 is generally the only one of practical importance. Usually the parametric resonance of the first kind is termed "parametric resonance", whereas the second kind is referred as "combination resonance", because it involves two different frequencies. In this paper the study is only concentrated in the case of parametric resonance.

Finding the boundaries of the regions of instability reduces to the determination of the conditions under which the differential equation (12) of the system has periodic solutions with period $2\pi/\varpi$ and $4\pi/\varpi$ (Bolotin, 1964). For the principal region, which is a half sub-harmonic, one looks for a solution with a period which is twice the forcing frequency: i.e., $4\pi/\varpi$.

The condition for the existence of solutions can be expressed in the following infinite determinant form (Bolotin, 1964).

$$\begin{vmatrix} \boldsymbol{K} - \boldsymbol{S}\left(P_s \pm \frac{1}{2}P_d\right) - \frac{1}{4}\varpi^2 \boldsymbol{M} & -\frac{1}{2}P_d \boldsymbol{S} & 0 & \cdots \\ & \boldsymbol{K} - P_s \boldsymbol{S} - \frac{9}{4}\varpi^2 \boldsymbol{M} & -\frac{1}{2}P_d \boldsymbol{S} & \cdots \\ sym & & \boldsymbol{K} - P_s \boldsymbol{S} - \frac{25}{4}\varpi^2 \boldsymbol{M} & \cdots \\ \cdots & \cdots & \cdots & \cdots \end{vmatrix} = 0 \tag{20}$$

The boundaries of the instability regions lying near the frequency $\varpi = 2\Omega$ can be determined with sufficient accuracy considering the first leading diagonal term:

$$\left|\boldsymbol{K} - \boldsymbol{S}\left(P_s \pm \frac{1}{2}P_d\right) - \frac{1}{4}\varpi^2 \boldsymbol{M}\right| = 0 \tag{21}$$

3.3 Influence of forced and parametrically excited vibrations

In the previous sections the longitudinal force in the beam is assumed equal to the external force acting at the end of the beam and therefore the longitudinal vibrations are neglected. Such an assumption is acceptable in certain bounds when the exciting frequency is small in comparison with the frequency ω_L of the free longitudinal vibrations. However for beams with small slenderness ratio or particular lamination sequence, the frequency at which a parametric resonance occurs, can be the same order as the natural frequency of the longitudinal vibrations. With the aim to include this effect in the analysis is necessary to substitute the constitutive expression corresponding to the axial force Q_x into the first differential equation in Eq (1) and solving for the displacement u, that is:

$$-J_{11}^{E}\frac{\partial^2 u}{\partial x^2} + J_{11}^{\rho}\frac{\partial^2 u}{\partial t^2} = 0 \tag{22}$$

Adopting the corresponding boundary condition, i.e. the first of Eq. (2), the solution to the Eq. (22) can be represented as:

$$u(x,t) = \frac{P_s x}{J_{11}^E} + \frac{P_d Sin[\eta.x]}{\eta J_{11}^E Cos[\eta.L]} Cos[\varpi.t] \tag{23}$$

where:

$$\eta = \varpi \sqrt{\frac{J_{11}^\rho}{J_{11}^E}} \tag{24}$$

Substituting the expression (23) into the remaining six differential equations given in the Eq. (1) and applying the same methodology previously explained, the equation (21) can be expressed in the following form:

$$\left| \boldsymbol{K} - \boldsymbol{S}\left(P_s \pm \frac{1}{2} P_d \frac{Tan[\eta.L]}{\eta.L} \right) - \frac{1}{4}\varpi^2 \boldsymbol{M} \right| = 0 \tag{25}$$

Now, solving Eq. (24) one can obtain the main regions of instability considering the influence of the longitudinal vibration.

4 APPLICATIONS AND NUMERICAL RESULTS

The scope of the section is to apply the aforementioned model in order to study the dynamic stability of simply-supported thin-walled composite beams with graded properties. The influence of longitudinal vibrations and the effect of shear deformation on the regions of instability are analyzed. When the beam is excited in the axial (longitudinal) direction, the interaction of this movement will depend on the symmetry of the cross-section analyzed. Different bisymmetrical cross-sectional shapes and beam lengths are considered to perform the numerical analysis. Variation of the volume fraction of ceramic through the thickness for the different values of volume fraction index is considered.

Among the many ways to characterize the law for graded material in this paper a simple gradation based in a power-law is employed. The Eq. (26) shows the law of variation of the elastic and mass properties along the wall-thickness *e*. This law of variation

$$\mathcal{P}(n) = \mathcal{P}_M + (\mathcal{P}_C - \mathcal{P}_M)\left(\frac{2n+e}{2e} \right)^K \tag{26}$$

where, $\mathcal{P}(n)$ denotes a typical material property (i.e., density ρ or Young's modulus E or Poisson coefficient ν). Sub-indexes C and M define the properties of the material of the outer surface (normally ceramic) and inner surface (normally metallic). The exponent K, which is connected to the ratio of constituents in volume, can have different values that may vary between zero (i.e., a full metallic phase) or infinity (i.e., a full ceramic phase). Figure 2 shows an example of properties gradation across the thickness for different values of the exponent K. Once the Young's modulus and Poisson coefficient are defined, it is possible to obtain the shear modulus and the elastic coefficient for a plane stress state (see Appendix I). The elastic and mass properties of the material constituents for Steel, Alumina, Aluminium and Silicon Carbide are summarized in Table 1.

In the following examples, that are associated with the cross-sections shown in Fig. 3, the system equations are uncoupled (because of the by-symmetry: $y_0 = z_0 = 0$). Therefore, there are three main modes of vibration corresponding either to bending or to torsion. In these cases, the lowest frequency corresponds to the lateral flexural mode (y-direction), while the highest vibration frequency corresponds to the twist mode. In all the results presented below,

the value of the static load parameter is adopted $\alpha = 0.5$, and the excitation frequency ϖ is scaled with the lowest frequency value of parametric resonance (i.e. the case when the value of the frequency associated to the first mode is doubled, or $\varpi = 2\Omega_1$).

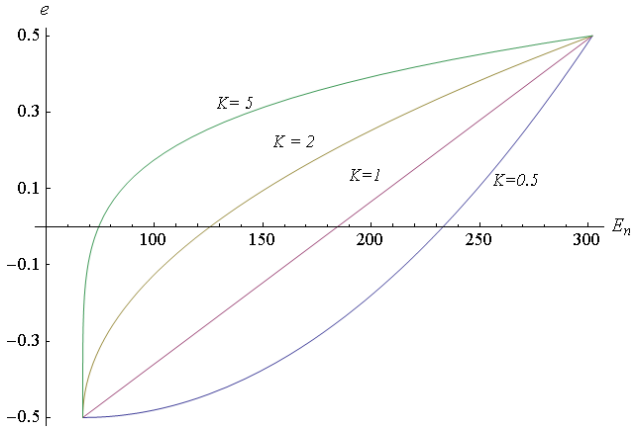

Figure 2: Example of properties gradation across the thickness.

Property	Steel	Alumina	Aluminium	Silicon Carbide
Young Modulus [GPa]	206	393	67	302
Poisson Coefficient	0.30	025	0.33	0.17
Density [Kg/m^3]	7800	3960	2700	3200

Table 1: Properties of Aluminium and Silicon Carbide.

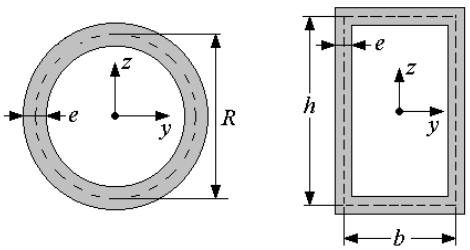

Figure 3: Cross-sectional cases to be evaluated.

4.1 Instability regions for different gradation intensity

The first example considered corresponds to a box section with the following geometrical properties: $L = 0.2$ m, $h/L = 0.05$, $b/h = 0.5$ and $e/h = 0.15$. The metallic material analyzed is aluminium and the fraction of the ceramic material is Silicon Carbide.

The first two instability regions corresponding to flexural vibration modes are shown in the Figure 4, for different values of volume fraction index K. The excitation frequency ϖ is scaled with the lowest frequency value of parametric resonance corresponding to $K = 10$. The natural frequencies in Hz are shown in Table 2, considering the dynamic load parameter $\beta = 0$. The frequency referred to the unloaded beam ($\alpha = 0$) is denoted by ω and Ω is the frequency when the beam is subjected to a static load ($\alpha = 0.5$). It is observed that the widest unstable region corresponds to the first mode (or to the main frequency of parametric resonance), while the smallest region belongs to the second mode (or second frequency of parametric resonance). The size of the unstable regions increases as decreases the value of volume fraction index K. The torsional parametric regions are very small and they are far away from the main unstable region. Besides, the influence of the longitudinal inertia is negligible in all

the cases analyzed, due to the exciting frequency is small in comparison to the frequency ω_L of the free longitudinal vibrations. This behavior can be observed from the frequencies relation shown in Table 2. It can be noted from Table 2, that the vibration frequency values (ω) decrease for a given static load parameter. This decrease is about 30% for the first flexural mode, 10% for the second vertical mode and 0.5% for the torsional mode. This effect keeps constant for the three cases of K analyzed. Figure 5 shows the variation of the vibration frequency values in function on the static load, corresponding to the first flexural mode and for different values of volume fraction index K. The higher value of static load, when the frequency value is $\Omega = 0$, correspond to the value of buckling load. In this case, the critical load of the beam corresponding to the flexural mode can be easily obtained by means of the following expression (as explained by Machado and Cortínez, 2005):

$$P_{CR} = \frac{\pi^2}{L^2} \frac{J_{33}^E J_{55}^E}{J_{55}^E + J_{33}^E \dfrac{\pi^2}{L^2}} \tag{27}$$

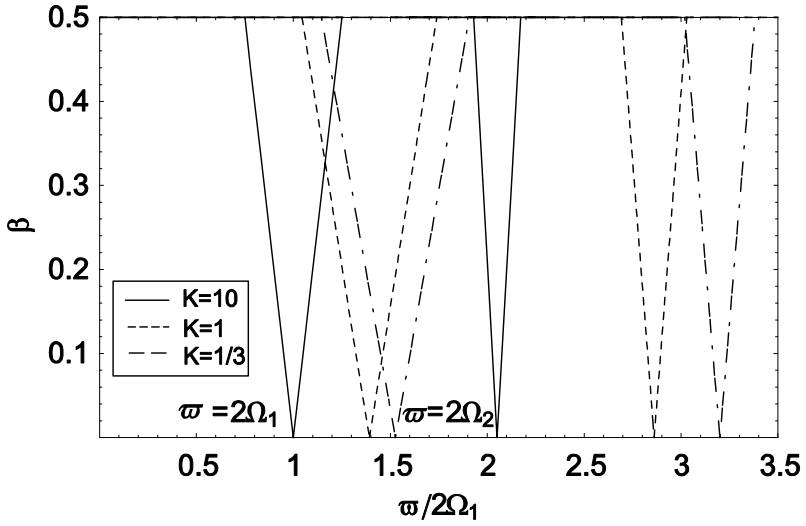

Figure 4: Comparison of the unstable regions for different values of K.

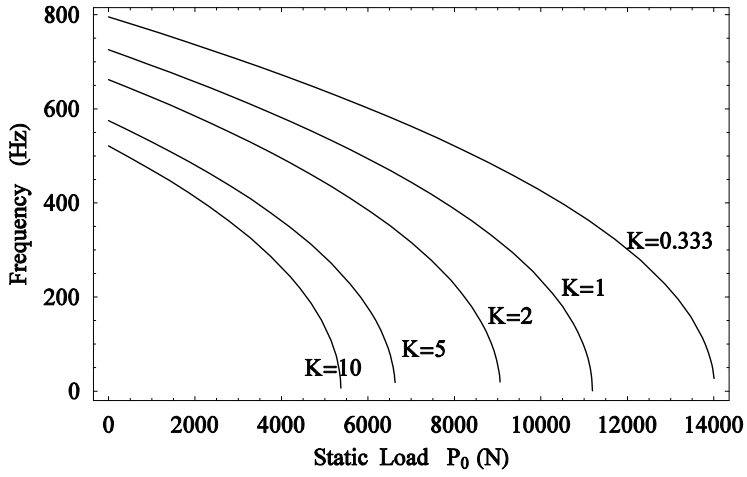

Figure 5: Variation of frequency values versus the static load for different values of K.

K	Modes	ω_i	Ω_i	ω_L
10	1	521.14	368.5	7095.21
	2	840.89	756.04	
	3	7632.03	7622.76	
1	1	725.46	512.97	9885.46
	2	1172.20	1054.26	
	3	10860.40	10847.80	
1/3	1	795.38	562.42	11118.83
	2	1306.18	1179.18	
	3	11843.10	11829.60	

Table 2: Natural frequencies for a box beam (*Hz*), L = 0.2m.

4.2 Instability regions: influence of longitudinal vibration

The second example corresponds to a box section with the following geometrical properties L = 0.5 m, h/L= 0.1, b/h = 0.5 and e/h = 0.1. The material properties are the same as the previous example. The regions of dynamic instability for the first two frequencies of vibration excited parametrically (Ω_1 and Ω_2) are shown in the Figure 6. The first region corresponds to the flexural mode in the lateral direction, while the second flexural mode is in vertical direction. The third region that appears in the figures represents the influence of the longitudinal vibration, which in this case is near to the parametric unstable boundaries. Comparative results are shown in Figure 6, between the unstable regions obtained by disregarding and considering the influence of the longitudinal vibration. It can be observed that the size of the unstable region is hardly the same for both models. In this example, the influence of the volume fraction index K was considered as in the previous example. However, the dynamical behavior observed for the three cases studied (K = 10, K = 1 and K = 1/3) was very similar, as in the previous case. Therefore, the unstable regions presented in Figure 6 correspond to a volume fraction index K=1.

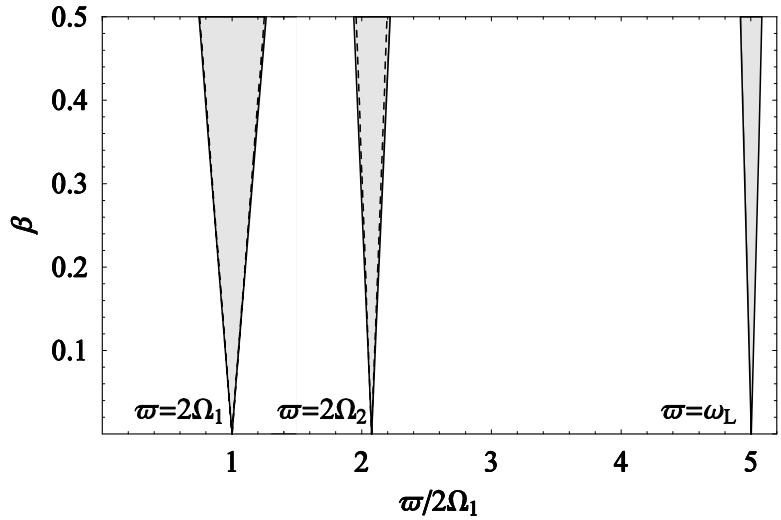

Figure 6: Unstable dynamic regions, (—) considering and (---) neglecting longitudinal inertia, for K=1.

The relation between the natural and the parametric excited frequencies values can be observed from Table 3, considering the dynamic load parameter β = 0. The variation of the frequency values in function of the static load is the same as the previous first example, where the first flexural mode presents the higher decrease (about 30%).

K	Modes	ω_i	Ω_i	ω_L
10	1	400.48	283.18	2838.08
	2	651.72	587.51	
	3	2924.39	2910.19	
1	1	558.49	394.92	3954.19
	2	909.42	819.94	
	3	4175.46	4156.13	
1/3	1	617.69	436.78	4447.23
	2	1017.09	919.35	
	3	4609.14	4588.08	

Table 3: Natural frequencies for a box beam (*Hz*), L = 0.5 m.

4.3 Instability regions: influence of longitudinal vibration; more parametric analysis

In this example the influence of the longitudinal inertia is analyzed for a box section with the geometrical properties L = 0.5 m, h/L= 0.15, considering two different relations of b/h = {0.5, 0.75} and e/h = {0.15, 0.05}. The material properties are the same as the previous examples and the volume fraction index considered is K=1. The regions of dynamic instability for the first two frequencies of vibration excited parametrically (Ω_1 and Ω_2) are shown in the Figures 7 and 8, for b/h = 0.5, e/h = 0.15 and b/h = 0.75, e/h = 0.05, respectively. Figures 7 and 8 show comparative results between the unstable regions obtained by considering (solid line) and disregarding (dashed line) the influence of the longitudinal vibration. It can be observed that the larger size correspond to the main unstable region ($2\Omega_1$) in comparison with the second ($2\Omega_2$) and third (ω_L) unstable region. The influence of the longitudinal inertia enlarges the unstable parametric regions. Therefore, its discard results, inadvertently, in a less critical behavior than in the case of its incorporation. The interaction of forced and parametrically excited vibrations is more noticeable for the second cross-section analyzed (Figure 8). It is due to the nearness of the longitudinal frequency value with the excited parametrically frequency values. The natural frequencies in Hz are shown in Table 4, for the unloaded beam $\alpha = 0$ and for $\alpha = 0.5$, considering the dynamic load parameter $\beta = 0$.

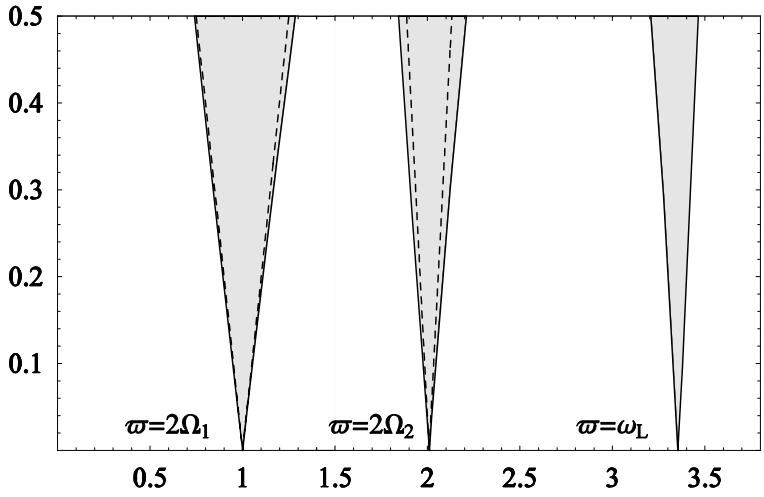

Figure 7: Unstable dynamic regions, (—) considering and (---) neglecting longitudinal inertia, for b/h = 0.5, e/h = 0.15.

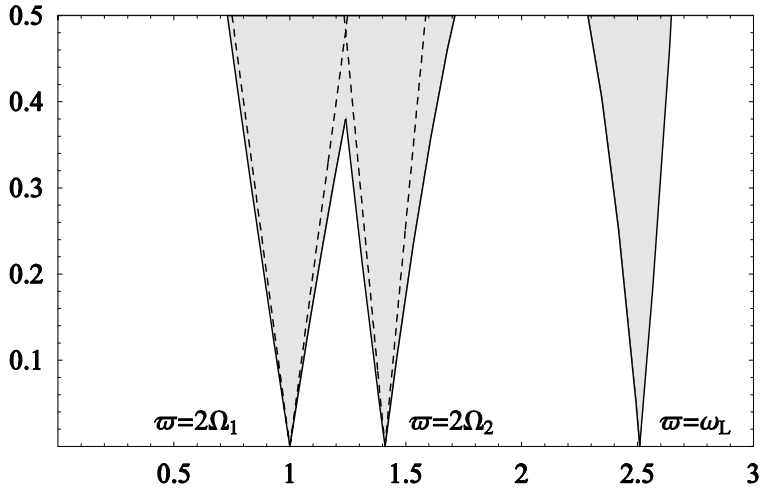

Figure 8: Unstable dynamic regions, (—) considering and (---) neglecting longitudinal inertia, for $b/h = 0.75$, $e/h = 0.05$.

K	Modes	ω_i	Ω_i	ω_L
$b/h = 0.5$ $e/h = 0.15$	1	834.38	590.00	3954.19
	2	1324.43	1187.98	
	3	4346.94	4304.79	
$b/h = 0.75$ $e/h = 0.05$	1	1113.94	787.69	3954.19
	2	1359.66	1110.63	
	3	4391.99	4318.46	

Table 4: Vibration frequencies for a box beam (*Hz*), $L = 0.5$m and $h/L = 0.15$.

4.4 Instability regions: influence of shear flexibility

The influence of shear deformation on the dynamic behavior is analyzed in this example. The geometrical properties corresponding to a box beam are $L = 0.5$ m, $h/L = 0.15$, $b/h = 0.5$ and $e/h = 0.1$. The material properties are the same as the previous examples. In Table 5, natural frequencies are given considering two models: the present theory (Model I) and neglecting shear flexibility (Model II). The shear deformation effect reduces the vibration frequency values. The same behavior is observed for the two cases analyzed (K=1 and K=1/3). The effect of shear flexibility on the unstable regions is shown in Figure 9, for a volume fraction index K=1. It is observed that the width of the regions does not change for both models. However, when shear deformation is neglected the unstable region moves toward the right, originated by an increase in the parametric frequency values.

K	Modes	ω_i		Ω_i	
		Model I	*Model II*	*Model I*	*Model II*
1	1	817.06	850.96	577.75	625.20
	2	1315.75	1386.52	1184.26	1263.20
	3	4177.29	4177.34	4135.66	4135.70
1/3	1	904.75	940.19	639.75	689.43
	2	1472.88	1549.39	1329.05	1414.18
	3	4611.46	4611.53	4565.99	4566.06

Table 5: Shear deformation effect on natural frequencies (*Hz*).

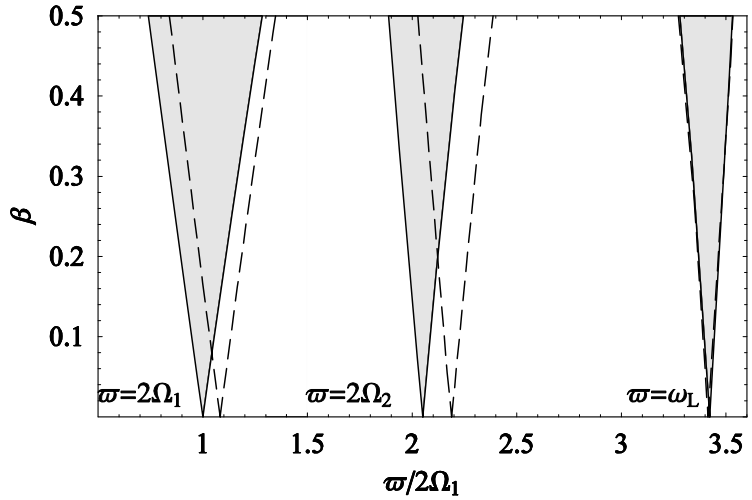

Figure 9: unstable dynamic regions, (—) considering and (- - -) neglecting shear deformation, for K=1.

4.5 Instability regions: circular beam

The example considered is a circular section with the geometrical properties L = 0.2 m, R/L= 0.15 and e/R = 0.05. The metallic material analyzed is steel and the fraction of the ceramic material is Alumina. Instability regions are shown in Figure 10, considering a volume fraction index K=1. The influence of the interaction between the forced vibration and the parametrically excited vibrations on the unstable regions is analyzed in the figure. The unstable boundaries obtained by disregarding this interaction are drawn in dashed lines. It is observed that the widest unstable region corresponds to the first and second flexural mode (or to the first and second frequencies of parametric resonance), while the smallest region corresponds to the torsional mode (or to the third frequency excited parametrically). In this case, the natural frequency corresponding to the longitudinal mode ω_L is next to the first parametric resonance frequency $2\Omega_1$.

K	Modes	ω_i	Ω_i	ω_L
10	1	5693.40	4028.07	10951.4
	2	5693.40	4028.07	
	3	13656.30	13020.0	
1	1	6138.16	4342.76	11766.6
	2	6138.16	4342.76	
	3	14817.61	14135.30	
1/3	1	6337.92	4484.09	12141.45
	2	6337.92	4484.09	
	3	15327.10	14624.50	

Table 6: Natural frequencies for a circular beam (*Hz*).

The influence of the longitudinal inertia enlarges the first region to the right, which seen to be composed by two regions. The first unstable region ($2\Omega_1$ and $2\Omega_2$) is smaller when the interaction of the forced vibration is omitted, predicting a less critical behavior. However, the third unstable region ($2\Omega_3$) is larger when the interaction of the forced vibration is omitted, predicting a more conservative behavior. The interaction of forced and parametrically excited vibrations is the same for the three material configurations analyzed (K). This behavior can be seen from Table 6, where the natural frequencies are shown for the case of the dynamic load parameter $\beta = 0$. The frequencies referred to the unloaded beam ($\alpha = 0$) are denoted by ω and

by Ω when the beam is subjected to a static load ($\alpha = 0.5$).

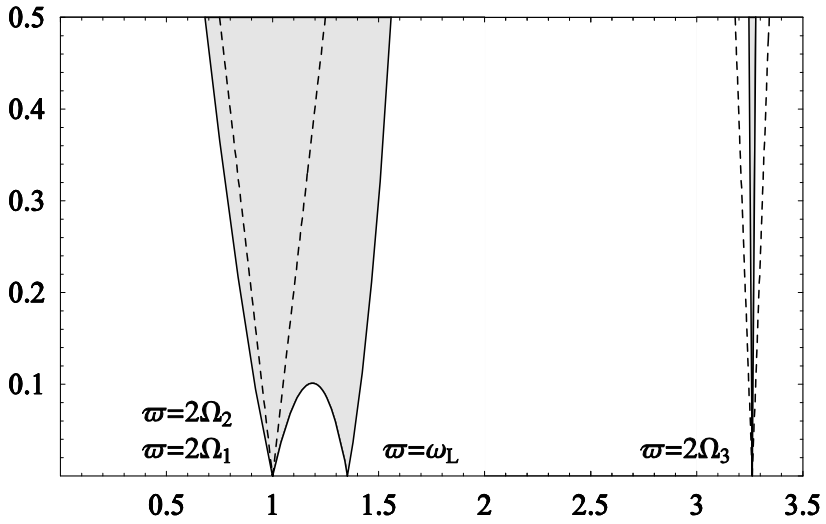

Figure 10: Unstable dynamic regions, (—) considering and (---) neglecting longitudinal inertia, for *K*=1.

5 CONCLUSIONS

The dynamic stability behavior of functionally graded thin-walled beams subjected to axial external force is investigated considering the influence of non conventional effects. The material properties of the functionally graded beam are assumed to vary continuously through the thickness, according to a simple power law distribution of the volume fraction of the constituents. The formulation is based on the context of a rational small strain and moderate rotation theory of thin-walled beams. The dynamic stability analysis of a simply supported beam subjected to an axial periodic force system is performed by employing the Hill's method of infinite determinants developed by Bolotin. The effects of shear deformation, volume fraction index and the interaction between forced and parametrically excited vibrations on the boundaries of the unstable regions are investigated.

From the numerical results obtained, it is found that the regions of instability dynamic are generally wider for the first frequency of parametric resonance. Besides, the size of the unstable regions can vary depending on the volume fraction index K, observing that it increases as decreases the value of K. The interaction between the forced vibration and the parametrically excited vibrations on the unstable regions is considerable when the excitation frequency is the same order than the frequency value of the free longitudinal vibration. Moreover, the influence of the longitudinal inertia enlarges the main parametric regions. This effect keeps constant for the three material configurations analyzed. On the other hand, the shear deformation effect reduces the vibration frequency values and this effect remains constant as increase the dynamical load parameter. The refuse of transverse shear leads to an overprediction of the resonance behavior, in the sense of the shift of the domain of instability toward larger excitation frequencies. Finally, in a future work the effect of temperature-dependent will be considered on the instability behavior of functionally graded thin-walled beams.

ACKNOLEDGMENTS

The support of Universidad Tecnológica Nacional, CONICET and ANPCYT is recognized.

REFERENCES

V.V. Bolotin, *The Dynamic Stability of Elastic Systems*, Holden-Day, San Francisco, 1964.

A. Chakraborty, S. Gopalakrishnan, J.N. Reddy. A new beam finite element for the analysis of functionally graded materials. *International Journal of Mechanical Sciences*, 45:519–539, 2003.

V.H. Cortínez and M.T. Piovan. Stability of composite thin-walled beams with shear deformability. *Computers and Structures*, 84:978-990, 2006.

H.J. Ding, D.J. Huang, W.Q. Chen. Elasticity solutions for plane anisotropic functionally graded beams. *International Journal of Solids and Structures,* 44:176–196, 2007

N. El-Abbasi, S.A. Meguid. Finite element modeling of the thermoelastic behavior of functionally graded plates and shells. *International Journal of Computer Engineering Science,* 1(1):151–65, 2000.

A.J. Goupee, S.S. Vel. Optimization of natural frequencies of bidirectional functionally graded beams. *Structural and Multidisciplinary Optimization,* 32 (6), 473–484, 2006

S. Kitipornchai, J. Yang, K.M. Liew. Semi-analytical solution for nonlinear vibration of laminated FGM plates with geometric imperfections. *International Journal of Solids and Structures* 41, (9–10):2235–2257, 2004.

S. Krenk, O. Gunneskov. Statics of thin-walled pre-twisted beams. *International Journal of Numerical Methods in Engineering* 17, 1407–1426, 1981.

S.P. Machado, Geometrically non-linear approximations on stability and free vibration of composite beams. *Engineering Structures,* 29(12): 3567-3578, 2008.

S.P. Machado, C.P. Filipich, V.H. Cortínez. Parametric vibration of thin-walled composite beams with shear deformation. *Journal of Sound and Vibration,* 305(4-5):563-581, 2007.

S.P. Machado, V.H. Cortínez. Non-linear model for stability of thin-walled composite beams with shear deformation. *Thin-Walled Structures,* 43(10):1615-1645, 2005.

R. Naj, M. Sabzikar Boroujerdy, M.R. Eslami. Thermal and mechanical instability of functionally graded truncated conical shells. *Thin-Walled Structures,* 46:65-78, 2008.

A.H. Nayfeh, D.T. Mook, *Nonlinear Oscillations*, Wiley, New York, 1979.

S-Y Oh, L. Librescu, O. Song. Thermoelastic modeling and vibrations of functionally graded thin-walled rotating blades. *AIAA Journal,* 41 (10):2051–60, 2003.

S-Y Oh, L. Librescu, O. Song. Vibration and instability of functionally graded circular cylindrical spinning thin-walled beams. *Journal of Sound and Vibration* 285(4-5):1071-1091, 2005.

M.T. Piovan and V.H. Cortínez. Mechanics of shear deformable thin-walled beams made of composite materials. Thin-Walled Structures 45:37–62, 2007.

G.N. Praveen, J.N. Reddy. Nonlinear transient thermoelastic analysis of functionally graded ceramic–metal plates. *International Journal of Solids Structures,* 35(33):4457–76, 1998.

J.N. Reddy, C.D. Chin. Thermomechanical analysis of functionally graded cylinders and plates. *Journal of Thermal Stresses,* 26(1):593–626, 1998.

J.N. Reddy. Analysis of functionally graded plates. *International Journal of Numerical Methods in Engineering,* 47:663–84, 2000.

H.J. Xiang, J. Yang. Free and forced vibration of laminated FGM Timoshenko beam of variable thickness under heat conduction. *Composites, Part B* 39:292-303, 2008.

J. Yang, Y. Chen. Free vibration and buckling analysis of functionally graded beams with edge cracks. *Composite Structures,* 83: 48-60, 2008.

K. Washizu. *Variational Methods in Elasticity and Plasticity*. Pergamon Press, 1974.

APPENDIX I: CONSTITUTIVE LAW

The constitutive laws for functionally graded structures are obtained by employing the assumptions of plane stress state in the thickness of the walls and a general transverse isotropy along the hook co-ordinate. Thus, once the longitudinal (E) and transversal elasticity modulus (G) and the Poisson's coefficient (ν) are given in a certain functional form, then the stresses in the wall can be described in the following form:

$$\begin{Bmatrix} \sigma_{xx} \\ \sigma_{ss} \\ \sigma_{xs} \end{Bmatrix} = \begin{bmatrix} Q_{11} & Q_{12} & 0 \\ Q_{12} & Q_{11} & 0 \\ 0 & 0 & Q_{66} \end{bmatrix} \begin{Bmatrix} e_{xx} \\ e_{ss} \\ e_{xs} \end{Bmatrix} \tag{I.1}$$

being:

$$Q_{11} = \frac{E_n}{1-\nu_n^2} \quad Q_{12} = \frac{E_n \nu_n}{1-\nu_n^2} \quad Q_{66} = \frac{E_n}{2(1+\nu_n)} \tag{I.2}$$

where, E_n, G_n and ν_n are the effective longitudinal modulus, transversal modulus and Poisson coefficient at a given co-ordinate in the thickness, respectively. These entities are defined according to certain gradation law that can be defined by means of a power law form or exponential form or any other that fits experimental data. The symbols e_{xx}, e_{ss} and e_{xs} intend for longitudinal, hook and tangential strains, respectively; and can be represented in terms of the shell strains as:

$$e_{xx} = \varepsilon_{xx} + n\kappa_{xx} \quad e_{ss} = \varepsilon_{ss} + n\kappa_{ss} \quad e_{xs} = \gamma_{xs} + n\kappa_{xs} \tag{I.3}$$

where ε_{xx}, ε_{ss} and γ_{xs} are longitudinal, hook and tangential shell strains, respectively and κ_{xx}, κ_{ss} and κ_{xs} are the corresponding curvatures.

Now employing the conventional definitions for shell-stress-resultants given by:

$$\begin{aligned} N_{xx} &= \int_{-e/2}^{e/2} \sigma_{xx} dn \qquad N_{ss} = \int_{-e/2}^{e/2} \sigma_{ss} dn \qquad N_{xs} = \int_{-e/2}^{e/2} \sigma_{xs} dn \\ M_{xx} &= \int_{-e/2}^{e/2} \sigma_{xx} n dn \quad M_{ss} = \int_{-e/2}^{e/2} \sigma_{ss} n dn \quad M_{xs} = \int_{-e/2}^{e/2} \sigma_{xs} n dn \end{aligned} \tag{I.4}$$

and integrating along the shell thickness e, one obtains the following expression:

$$\begin{Bmatrix} N_{xx} \\ N_{ss} \\ N_{xs} \\ M_{xx} \\ M_{ss} \\ M_{xs} \end{Bmatrix} = \begin{bmatrix} A_{11} & A_{12} & 0 & B_{11} & B_{12} & 0 \\ & A_{11} & 0 & B_{12} & B_{11} & 0 \\ & & A_{66} & 0 & 0 & B_{66} \\ & & & D_{11} & D_{12} & 0 \\ & sym & & & D_{11} & 0 \\ & & & & & D_{66} \end{bmatrix} \begin{Bmatrix} \varepsilon_{xx} \\ \varepsilon_{ss} \\ \gamma_{xs} \\ \kappa_{xx} \\ \kappa_{ss} \\ \kappa_{xs} \end{Bmatrix} \tag{I.5}$$

where:

$$A_{ij} = \int_{-e/2}^{e/2} Q_{ij} dn \quad B_{ij} = \int_{-e/2}^{e/2} Q_{ij} n dn \quad D_{ij} = \int_{-e/2}^{e/2} Q_{ij} n^2 dn \tag{I.6}$$

Now assuming that $N_{ss} \cong 0$ and $M_{ss} \cong 0$ and rearranging ε_{ss} and κ_{ss} in the remaining equations one obtains the modified constitutive law for shell forces and moments as it is given in the Eq. (5):

$$\begin{Bmatrix} N_{xx} \\ N_{xs} \\ M_{xx} \\ M_{xs} \end{Bmatrix} = \begin{bmatrix} \overline{A}_{11} & 0 & \overline{B}_{11} & 0 \\ 0 & \overline{A}_{66} & 0 & \overline{B}_{66} \\ \overline{B}_{11} & 0 & \overline{D}_{11} & 0 \\ 0 & \overline{B}_{66} & 0 & \overline{D}_{66} \end{bmatrix} \begin{Bmatrix} \varepsilon_{xx} \\ \gamma_{xs} \\ \kappa_{xx} \\ \kappa_{xs} \end{Bmatrix} \tag{I.7}$$

where $\overline{A}_{66} = A_{66}$, $\overline{B}_{66} = B_{66}$, $\overline{D}_{66} = D_{66}$ and

$$\begin{aligned} \overline{A}_{11} &= A_{11} + \left(2A_{12}B_{11}B_{12} - A_{11}B_{12}^2 - A_{12}^2 D_{11}\right)/\Delta \\ \overline{B}_{11} &= B_{11} + \left(B_{11}B_{12}^2 + A_{12}B_{11}D_{12} - A_{11}B_{12}D_{12} - A_{12}B_{12}D_{11}\right)/\Delta \\ \overline{D}_{11} &= D_{11} + \left(2D_{12}B_{11}B_{12} - A_{11}D_{12}^2 - B_{12}^2 D_{11}\right)/\Delta \\ \Delta &= D_{11}A_{11} - B_{11}^2 \end{aligned} \tag{I.8}$$

In order to obtain an expression of the generalized forces in terms of the generalized strains, one has to consider that the shell strains of Eq. (I.7) can be expressed in the following form (Machado et al, 2007):

$$\begin{aligned} \varepsilon_{xx} &= \varepsilon_{D1} + \overline{Z}\varepsilon_{D2} + \overline{Y}\varepsilon_{D3} + \omega_p \varepsilon_{D4} + \left(Y^2 + Z^2\right)\varepsilon_{D9} \\ \gamma_{xs} &= \frac{dY}{ds}\varepsilon_{D5} + \frac{dZ}{ds}\varepsilon_{D6} + \left(r(s) - \psi\right)\varepsilon_{D7} + \psi\varepsilon_{D8} \\ \kappa_{xx} &= \frac{dY}{ds}\varepsilon_{D2} - \frac{dZ}{ds}\varepsilon_{D3} - l(s)\varepsilon_{D4} - 2r\varepsilon_{D9} \\ \kappa_{xs} &= -2\varepsilon_{D8} \end{aligned} \tag{I.9}$$

where the generalized strains ε_{Di}, $i = 1,...,9$ are given as follows (Machado et al., 2007):

$$\begin{aligned} \varepsilon_{D1} &= u' + \frac{1}{2}\left(v'^2 + w'^2\right) + \phi_x\left(z_0\theta_z' - y_0\theta_y'\right) \\ \varepsilon_{D2} &= -\theta_y' + \theta_z'\phi_x \\ \varepsilon_{D3} &= -\theta_z' - \theta_y'\phi_x \\ \varepsilon_{D4} &= \theta_x' - \frac{1}{2}\left(\theta_z\theta_y'' - \theta_y\theta_z''\right) \\ \varepsilon_{D5} &= \left(v' - \theta_z\right) - \frac{z_0}{2}\left(\theta_z\theta_y' - \theta_y\theta_z'\right) \\ \varepsilon_{D6} &= \left(w' - \theta_z\right) + \frac{y_0}{2}\left(\theta_z\theta_y' - \theta_y\theta_z'\right) \\ \varepsilon_{D7} &= \phi_x' - \theta_x \\ \varepsilon_{D8} &= \phi_x' - \frac{1}{2}\left(\theta_z\theta_y' - \theta_y\theta_z'\right) \\ \varepsilon_{D9} &= \frac{\phi_x'^2}{2} \end{aligned} \tag{I.10}$$

Now taking into account the definition of the forces given in the Eq. (3) and employing the definitions of shell forces and strains given in Eqs (I.7), (I.9) and (I.10) one gets:

$$\boldsymbol{F} = \boldsymbol{J}^{\boldsymbol{E}}\boldsymbol{\Delta} \tag{I.11}$$

where the vectors of generalized forces $\boldsymbol{F}$ and generalized strains $\boldsymbol{\Delta}$ are:

$$\begin{aligned}\boldsymbol{F} &= \left\{Q_x \quad M_y \quad M_z \quad B \quad Q_y \quad Q_z \quad T_W \quad T_{SV} \quad B_W\right\}^T \\ \boldsymbol{\Delta} &= \left\{\varepsilon_{D1} \quad \varepsilon_{D2} \quad \varepsilon_{D3} \quad \varepsilon_{D4} \quad \varepsilon_{D5} \quad \varepsilon_{D6} \quad \varepsilon_{D7} \quad \varepsilon_{D8} \quad \varepsilon_{D9}\right\}^T\end{aligned} \tag{I.12}$$

The matrix $\boldsymbol{J}$ of rigidity coefficients is given by:

$$\boldsymbol{J}^{\boldsymbol{E}} = \int_S \boldsymbol{M}_D^T \boldsymbol{N}_P \boldsymbol{M}_D ds \tag{I.13}$$

Where

$$\boldsymbol{N}_P = \begin{bmatrix} \overline{A}_{11} & 0 & \overline{B}_{11} & 0 \\ 0 & \overline{A}_{66} & 0 & \overline{B}_{66} \\ \overline{B}_{11} & 0 & \overline{D}_{11} & 0 \\ 0 & \overline{B}_{66} & 0 & \overline{D}_{66} \end{bmatrix} \tag{I.14}$$

$$\boldsymbol{M}_D = \begin{bmatrix} 1 & \overline{Z} & \overline{Y} & \omega_p & 0 & 0 & 0 & 0 & Y^2+Z^2 \\ 0 & 0 & 0 & 0 & dY/ds & dZ/ds & r(s)-\psi & \psi & 0 \\ 0 & dY/ds & -dZ/ds & -l(s) & 0 & 0 & 0 & 0 & -2r(s) \\ 0 & 0 & 0 & 0 & 0 & 0 & 0 & -2 & 0 \end{bmatrix} \tag{I.15}$$

In the case of doubly symmetric thin-walled beam whose graded properties are distributed uniformly in the hook direction one can obtain the following matrix $\boldsymbol{J}^{\boldsymbol{E}}$:

$$\boldsymbol{J}^{\boldsymbol{E}} = \begin{bmatrix} J_{11}^E & 0 & 0 & 0 & 0 & 0 & 0 & 0 & J_{19}^E \\ & J_{22}^E & 0 & 0 & 0 & 0 & 0 & 0 & 0 \\ & & J_{33}^E & 0 & 0 & 0 & 0 & 0 & 0 \\ & & & J_{44}^E & 0 & 0 & 0 & 0 & 0 \\ & & & & J_{55}^E & 0 & 0 & 0 & 0 \\ & & & & & J_{66}^E & 0 & 0 & 0 \\ & & & & & & J_{77}^E & 0 & 0 \\ & & sym & & & & & J_{88}^E & 0 \\ & & & & & & & & J_{99}^E \end{bmatrix} \tag{I.16}$$

From the previous expressions one can obtain B_W in terms of Q_x by neglecting the effect of higher order strains in terms of the twisting angle gradient (Machado et al, 2007), leading to

$$B_W = Q_X \frac{J_{19}^E}{J_{11}^E} \tag{I.17}$$

This form is substituted in Eqs. (1) and (2), thus simplifying the problem.